

Thermal decomposition of surfactant coatings on Co and Ni nanocrystals

V. Pérez-Dieste, O. M. Castellini, J. N. Crain, M. A. Eriksson, A. Kirakosian, J.-L. Lin, J. L. McChesney, and F. J. Himpsel^{a)}

Department of Physics, University of Wisconsin Madison, Madison, Wisconsin 53706

C. T. Black and C. B. Murray

IBM T. J. Watson Research Center, Yorktown Heights, New York 10598

(Received 18 August 2003; accepted 22 October 2003)

The pathway for thermal decomposition of an oleic acid surfactant protecting Co and Ni nanocrystals is identified by probing the relevant molecular orbitals with x-ray absorption spectroscopy. The two steps observed previously in thermogravimetric measurements are identified with thermal desorption of entire molecules at $\approx 200^\circ\text{C}$ and dehydrogenation at $\approx 400^\circ\text{C}$, which leaves a graphitic surface with alkane fragments underneath. © 2003 American Institute of Physics. [DOI: 10.1063/1.1633971]

Synthesis methods for highly perfect nanocrystals use protective organic shells to achieve size distributions with a precision approaching that of a single atomic shell. Initially used for semiconductors¹ the method has been extended to magnetic materials, such as Co, Ni, and FePt.^{2–8} The monodispersity of the particles is highly attractive for designing magnetic storage media with fewer particles per bit without increasing fluctuations in the readout signal. In addition to aiding synthesis, the organic shell provides chemical stability to reactive transition metals,⁹ analogous to the use of a carbon coating.¹⁰ Furthermore, organic molecules act as tunable spacers preventing magnetic coupling between adjacent particles.

For magnetic storage applications, FePt particles need to be annealed to 560°C in order to transform them into the ordered face-centered-tetragonal phase with high coercivity.^{3,8} This leads to a decomposition of the organic shell, and the residue has been associated with a carbonaceous species.^{3,7} Its chemical nature and the reactions leading to it have not been identified. We apply near edge x-ray absorption spectroscopy (NEXAFS) with simultaneous electron and fluorescence detection to determine the changes in the chemical state of the organic shell during thermal decomposition. Specific chemical configurations are identified by their spectral signatures, such as the carboxylic acid group, the alkane backbone, and graphitic carbon. Two processes are found, i.e., partial desorption of the surfactant at low temperature ($\approx 200^\circ\text{C}$) and dehydrogenation at high temperature ($\approx 400^\circ\text{C}$). The former is evidenced by a decrease of all NEXAFS peaks characteristic of oleic acid, the latter by the loss of the hydrocarbon peaks and the dominance of the C=C π^* peak.

Beyond magnetic data storage it would be interesting to apply this method to reveal chemical driving forces during the self-assembly of nanocrystal arrays.^{2,8,11} For example, the thickness of the organic shell relative to the metallic core determines the crystal lattice of the array, as demonstrated for Fe and FePt nanocrystals coated with oleic acid and oleylamine.⁸ This ratio is proportional to the ratio of

the NEXAFS signals from carbon and the metal in the bulk-sensitive fluorescence mode. The organic shell can also be used as photoresist to pattern nanocrystal arrays by electron beam irradiation,¹² presumably by cleavage of C–H and C–C bonds. Such a reaction would exhibit a similar NEXAFS pattern as described here for the dehydrogenation of aliphatic bonds.

NEXAFS is a highly selective technique for sampling unoccupied orbitals at specific sites by observing optical transitions from a specific core level into the lowest unoccupied orbitals. Recently, the S 1s NEXAFS spectrum has been used to characterize alkanethiol-capped Pd and Au nanoparticles.^{13,14} We use transitions from the C 1s level to the π^* and σ^* orbitals and distinguish carbon atoms with different oxidation states by their C 1s shifts. Two detection methods are combined in order to separate surface from bulk effects, i.e., collecting electrons with an escape depth of ≈ 2 nm and detecting core level fluorescence with a mean free path of ≈ 100 nm. Both are decay products of the core hole and thus proportional to the number of absorbed photons.

The samples were Ni and Co nanocrystals (10 nm diameter) synthesized at IBM using techniques described previously.² The coating consists of oleic acid (see Fig. 1, bottom) with the aliphatic chain forming a hydrophobic coat. About 50%–60% of a monolayer of nanocrystals was deposited from a hexane or hexane/toluene solution by two methods. In the first method the substrate was soaked in the solution for a minimum of an hour and then rinsed in toluene. The second method used a variation of a Langmuir–Blodgett technique where the nanocrystal solution was floated on top of ethylene glycol and the silicon substrate touched the surface of the solution upside down. Rinsing in toluene eliminated excess glycol.

Specific molecular groups leave their fingerprints in the NEXAFS spectrum by a combination of the chemical shift of the core level and the empty valence level involved in the optical transition. Characteristic chemical groups can be identified using small molecules as models,^{15–17} as shown in Fig. 1. In general, the first peaks encountered above the C 1s absorption threshold are due to transitions from C 1s into π^* orbitals of C=C double bonds (f), including the π^* peak in

^{a)}Electronic mail: fhimpse@facstaff.wisc.edu

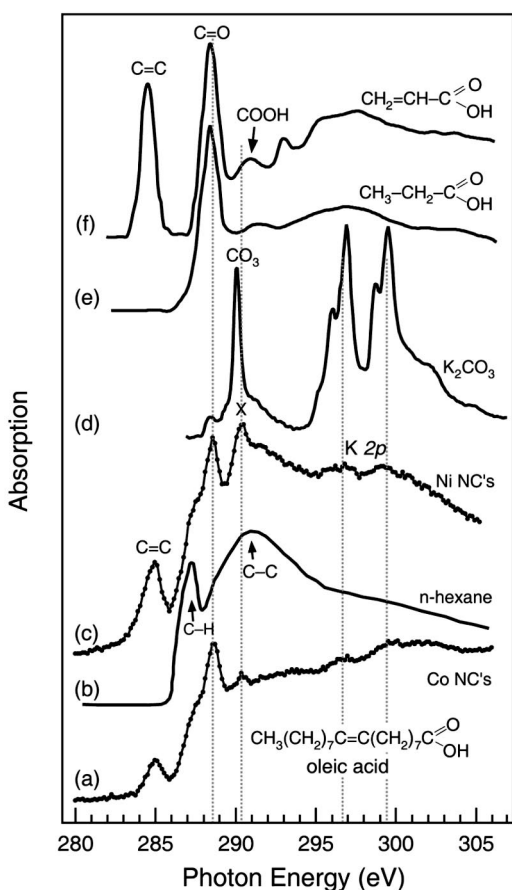


FIG. 1. Fingerprinting of molecular groups contained in the oleic acid coating of Ni and Co nanocrystals. Reference spectra from the literature are used to identify characteristic end groups, with (b) from Ref. 15, (d) from our work, and (e),(f) from Ref. 16.

graphitic carbon at 285 eV. Transitions to π^* orbitals are shifted up in energy at carbon atoms with $\text{C}=\text{O}$ double bonds because oxygen lowers the C 1s level by withdrawing electrons and lowering the electrostatic potential for the core electrons (e),(f). Additional electronegative ligands create transitions shifted up further,¹⁷ such as for CO_3 groups (d). These overlap with the lowest σ^* orbitals of C–C single bonds, but tend to be narrower than σ^* orbitals. The C–H orbitals of an alkane chain lie between the π^* peaks, for example a peak in hexane (b) and a corresponding shoulder in the nanocrystal spectra. Their weaker cross section demphasizes the contribution from the alkane backbone of oleic acid. The assignments are rather clear, except for the small peak labeled X. Associating it with the COOH group [Figs. 1(e) and 1(f)] would be consistent with the simultaneous intensity drop of X and the C=O peak during desorption (Figs. 2 and 3). Alternatively, the position and width of peak X would fit well to the dominant transition in carbonates (d), a possible impurity from processing oleic acid (see next).

An extra pair of unexpected peaks appears at about 297 and 299 eV in Fig. 1, significantly above the C 1s NEXAFS features. It occurs exclusively in bulk-like fluorescence spectra (Fig. 2, top). The characteristic spin-orbit splitting and binding energy give it away as K. There is a good match with our spectrum of K_2CO_3 in Fig. 1(d). In fact, K is used in manufacturing oleic acid via saponification of olive oil with KOH or K_2CO_3 .

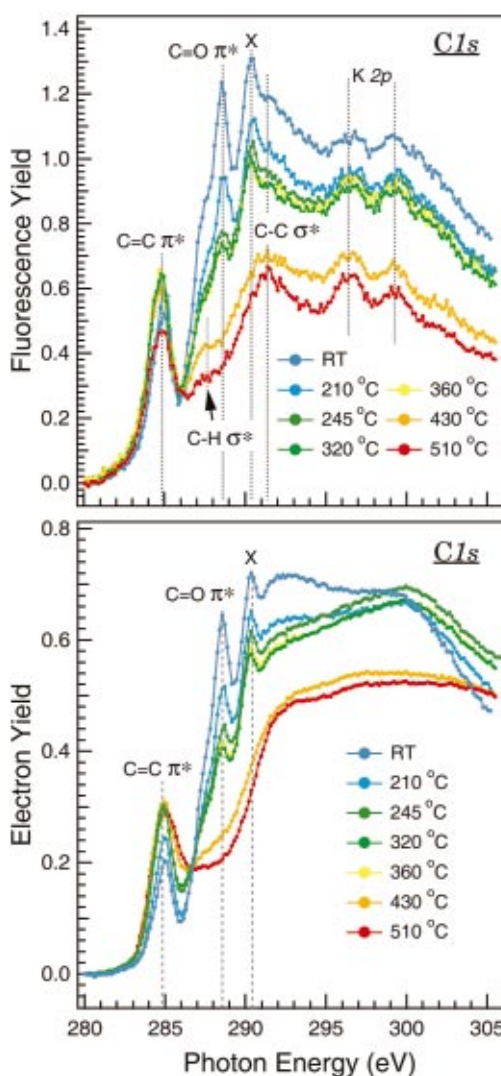


FIG. 2. (Color) C 1s absorption spectra versus annealing temperature for Ni nanocrystals coated with oleic acid. Detection of fluorescence photons probes the bulk (≈ 100 nm, top) and electron detection the surface (≈ 2 nm, right). The K impurity appears in the bulk only (Ref. 19).

The changes in the absorption spectrum during thermal decomposition of the organic shell are shown in Fig. 2 and quantified in Fig. 3 for specific peaks. All data have been normalized to the pre-edge background, and this constant background has been subtracted from the raw data. The remaining signal is proportional to the various hydrocarbon species. In both figures the top panel represents bulk-sensitive fluorescence and the bottom panel surface-sensitive electron yield. The annealing time was 10 s at each temperature step, using ohmic heating of the Si substrates in vacuum. The heating current provides fairly accurate relative temperatures but the overall calibration is uncertain by ± 50 °C when comparing the reading of a thermocouple with an infrared pyrometer.

A two-step reduction of the overall signal is observed, with a small drop between room temperature and 210 °C and a large drop between 360 and 430 °C (Fig. 2). A similar two-step process has been found in thermogravimetric measurements,⁹ where a small weight loss occurs at 240 °C (2.5%) and a larger loss at 380 °C (6.6%). The first step preserves the features of the NEXAFS spectra, indicating mainly thermal desorption of oleic acid. This is consistent with the

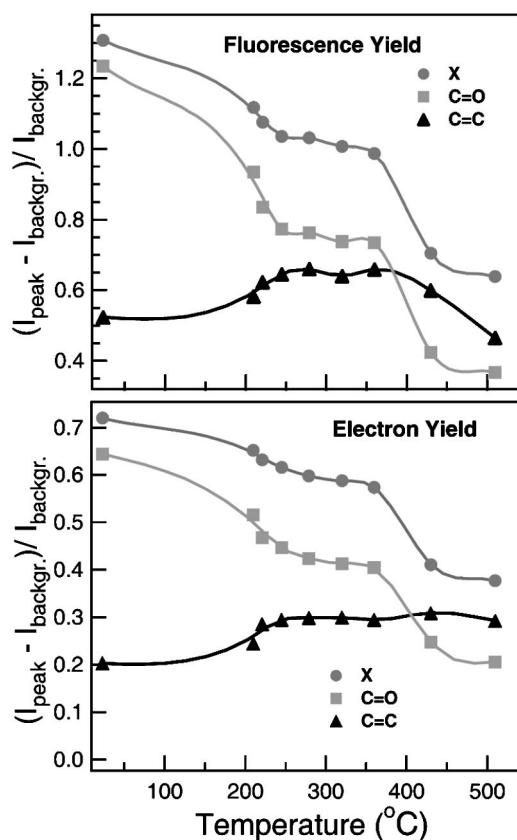


FIG. 3. Evolution of NEXAFS peak intensities corresponding to oleic acid (C=O and X=COOH or CO₃) vs double-bonded C=C. During heating the oleic acid signal decreases in two steps, due to desorption at $\approx 200^\circ\text{C}$ and via dehydrogenation at $\approx 400^\circ\text{C}$.

tent with a model where excess surfactant is bound weakly in a second layer.⁹ In the second step at $\approx 400^\circ\text{C}$ the sharp peaks related to oleic acid are completely removed and replaced by a single peak at 285 eV in the surface-sensitive electron spectra. It corresponds to the π^* peak of C=C double bonds in graphitic C and indicates a dehydrogenation of oleic acid, a reaction that is common to hydrocarbons adsorbed on transition metal catalysts, including Ni and Co. In the bulk-sensitive fluorescence spectra there is a remnant of the C-H and C-C features characteristic of alkanes, but the sharp π^* peaks of oleic acid have disappeared.

The integrated spectral weight of the C 1s spectrum provides a measure of the overall carbon content of the film. The surface-sensitive electrons still see 75% of the C signal within the outer 2 nm, while the bulk content of C in the nanocrystal film has decreased to about 50% when using the fluorescence signal. This is consistent with a model where the surfaces are still coated with a carbon layer while the overall amount of carbon in the film decreases by a factor of 2.

In summary, we show how NEXAFS with combined electron and fluorescence detection makes it possible to detect molecular orbitals of surfactant layers protecting nanocrystals. The change of the orbital structure during thermal decomposition reveals the relevant chemical reactions, both at the surface and in the bulk. The two stages of mass loss in thermogravimetric measurements are identified with thermal desorption of extra oleic acid layers at $\approx 200^\circ\text{C}$ and with dehydrogenation at $\approx 400^\circ\text{C}$, which leaves a graphitic surface with oleic acid fragmented into alkanes underneath. Our results can serve as a model for analyzing a variety of chemical reactions occurring between coated nanocrystals and surfaces, for example during patterning of self-assembled layers by UV, extreme UV, x ray, and e-beam lithography.^{12,18}

The authors acknowledge helpful suggestions from A. Hitchcock on the interpretation of the NEXAFS peaks and K. Pellerin's help with calibrating the temperature. This work was supported by the DOE under Contract No. DE-FG02-01ER45917. Additional support was provided by NSF DMR-0079983, DMR-0084402 (SRC), DMR-0094063, and DOE No. DE-AC03-76SF00098 (ALS).

¹C. B. Murray, D. J. Norris, and M. G. Bawendi, *J. Am. Chem. Soc.* **115**, 8706 (1993).

²S. Sun and C. B. Murray, *J. Appl. Phys.* **85**, 4325 (1999).

³S. Sun, C. B. Murray, D. Weller, L. Folks, and A. Moser, *Science* **287**, 1989 (2000).

⁴C. B. Murray, S. Sun, H. Doyle, and T. Betley, *MRS Bull.* **26**, 985 (2001).

⁵V. F. Puentes, K. M. Krishnan, and P. Alivisatos, *Appl. Phys. Lett.* **78**, 2187 (2001).

⁶S. Yamamuro, D. F. Farrell, and S. A. Majetich, *Phys. Rev. B* **65**, 224431 (2002).

⁷B. Stahl, J. Ellrich, R. Theissmann, M. Ghafari, S. Bhattacharya, H. Hahn, N. S. Gajbhiye, D. Kramer, R. N. Viswanath, J. Weissmüller, and H. Gleiter, *Phys. Rev. B* **67**, 014422 (2003).

⁸Y. Ding, S. Yamamuro, D. Farrell, and S. A. Majetich, *J. Appl. Phys.* **93**, 7411 (2003).

⁹Y. Sahoo, H. Pizem, T. Fried, D. Golodnitsky, L. Burstein, C. N. Suenik, and G. Markovich, *Langmuir* **17**, 7907 (2001).

¹⁰Y. D. Zhang, J. I. Budnick, W. A. Hines, S. A. Majetich, and E. M. Kirkpatrick, *Appl. Phys. Lett.* **76**, 94 (2000).

¹¹X. M. Lin, H. M. Jaeger, C. M. Sorensen, and K. J. Klabunde, *J. Phys. Chem. B* **105**, 3353 (2001).

¹²X. M. Lin, R. Parthasarathy, and H. M. Jaeger, *Appl. Phys. Lett.* **78**, 1 (2001).

¹³P. Zhang and T. K. Sham, *Appl. Phys. Lett.* **82**, 1778 (2003).

¹⁴P. Zhang and T. K. Sham, *Phys. Rev. Lett.* **90**, 245502 (2003).

¹⁵A. P. Hitchcock and I. Ishii, *J. Electr. Spectrosc. Relat. Phenom.* **42**, 11 (1987).

¹⁶I. Ishii and A. P. Hitchcock, *J. Electr. Spectrosc. Relat. Phenom.* **46**, 55 (1988).

¹⁷S. G. Urquhart and H. Ade, *J. Phys. Chem. B* **106**, 8531 (2002).

¹⁸S. O. Kim, H. H. Solak, M. P. Stoykovich, N. J. Ferrier, J. J. de Pablo, and P. F. Nealey, *Nature (London)* **424**, 411 (2003).

¹⁹Fluorescence is actually somewhat less sensitive to K 2p than to C 1s, judging from calculated cross section ratios for fluorescence/Auger decay of a K 2p versus a C 1s core hole.